V. SUPPLEMENTARY MATERIALS

A. Table of key terms

A table of key terms can be found in Table I.

B. Effective information calculation

Mathematically, EI has been expressed in a number of previous ways. The first was as the mutual information between two subsets of a system (while injecting noise into one), originally proposed as a step in the calculation of integrated information between neuron-like elements [47, 48]. More recently, it was pointed out that in general an intervention distribution, I_D, defined as a probability distribution over the $do(x)$ operator (as in [14]), creates some resultant effect distribution, E_D. Then the EI is the mutual information, $I(I_D; E_D)$, between the two, when the interventions are done like a randomized trial to reveal the dependencies (i.e., at maximum entropy [16, 49]).

In order to calculate the total information contained in the causal relationships of a system, EI is applied to the system as a whole [11]. There, EI was defined over the set of all states of a system and its state transitions. Because the adjacency matrix of a network can be cast as a transition matrix (as in Fig. 7a), the EI of a network can be expressed as:

$$EI = \frac{1}{N}\sum_{i=1}^{N} \mathrm{D}_{KL}[W_i^{out} || \langle W_i^{out} \rangle] \tag{7}$$

where EI is the average of the *effect information*, EI_i, of each node (see Table I and Fig. 7b). This is equivalent to our derivation of EI from first principles in Equation 1, since:

$$\begin{aligned} EI &= \frac{1}{N}\sum_{i=1}^{N} \mathrm{D}_{KL}[W_i^{out} || \langle W_i^{out} \rangle] \\ &= \frac{1}{N}\sum_{i=1}^{N}\sum_{j=1}^{N} w_{ij}\log_2\left(\frac{w_{ij}}{W_j}\right) \\ &= \frac{1}{N}\sum_{i=1}^{N}\left(\sum_{j=1}^{N} w_{ij}\log_2(w_{ij}) - \sum_{j=1}^{N} w_{ij}\log_2(W_j)\right) \\ &= \frac{1}{N}\sum_{i=1}^{N}\sum_{j=1}^{N} w_{ij}\log_2\left(w_{ij}\right) - \frac{1}{N}\sum_{i=1}^{N}\sum_{j=1}^{N} w_{ij}\log_2\left(W_j\right) \end{aligned} \tag{8}$$

Note that for a given node, v_i, the term in the first summation in Equation 8 above, $\sum_{j=1}^{N} w_{ij}\log_2\left(w_{ij}\right)$, is equivalent to the negative entropy of the out-weights from v_i, $-H(W_i^{out})$. Also note that W_j, the jth element in the $\langle W_i^{out} \rangle$ vector, is the normalized sum of the incoming weights to v_j from its neighbors, v_i, such that $W_j = \frac{1}{N}\sum_{i=1}^{N} w_{ij}$. We substitute these two terms into Equation 8 above such that:

$$EI = \frac{1}{N}\sum_{i=1}^{N} -H(W_i^{out}) - \sum_{j=1}^{N} W_j \log_2\left(W_j\right) \tag{9}$$

This is equivalent to the formulation of EI from Equation 1, since $H(\langle W_i^{out} \rangle) = -\sum_{j=1}^{N} W_j \log_2(W_j)$:

$$EI = H(\langle W_i^{out} \rangle) - \langle H(W_i^{out}) \rangle \tag{1}$$

In the derivations of SM V C we adopt the relative entropy formulation of EI from Equation 7 for ease of derivation. For a visual intuition behind the calculations involved in this formulation of EI, see how the network in Fig. 7a is used to calculate its EI (Fig. 7b), by calculating the mean effect information, EI_i, of nodes in the network.

C. Deriving the effective information of common network structures

Here we inspect the EI for iconic graphical structures, and in doing so, we see several interesting relationships between a network structure and its EI. First, however, we will introduce key terminology and assumptions.

Let $\langle k \rangle$ be the average degree of a network, G, and each node, v_i, has degree, k_i. In directed graphs each v_i has an in-degree, k_i^{in}, and an out-degree, k_i^{out}. These correspond to the number of edges leading in to v_i and edges going out from v_i. The total number of edges in G is represented by E. In undirected Erdős-Rényi (ER) networks, the total number of edges is given by $E = p\frac{N(N-1)}{2}$, where p represents the probability that any two nodes, v_i and v_j, will be connected. In the following subsections, we derive the EI of several prototypical network structures, from random graphs to ring lattices to star networks. Note that for the following derivations we proceed from the relative entropy formalism from SM V B, and note that therefore N is the number of nodes with the output, $N = N_{out}$.

1. *Derivation: effective information of ER networks*

In Erdős-Rényi networks, EI does not depend on the number of nodes in the network, N. Instead, the network's EI reaches its maximum at $-\log_2(p)$. This is because in ER networks, each node is expected to connect to $\langle k \rangle = pN$ neighboring nodes, such that every value

Term	Description	Notation
Network size	the number of nodes in the network	N
Out-weight vector (v_i)	a vector of probabilities w_{ij} that a random walker on node v_i will transition to v_j	$W_i^{out} = \{w_{i1}, w_{i2}, , ...w_{ij}, ...w_{iN}\}$
Effective information (network)	the total information in a causal structure, in bits	$EI = H(\langle W_i^{out}\rangle) - \langle H(W_i^{out})\rangle$
Determinism (v_i)	how certain about next steps is a random walker on v_i	$\det_i = \log_2(N) - H(W_i^{out})$
Degeneracy (network)	how distributed the certainty is over the nodes of the network	$\text{degeneracy} = \log_2(N) - H(\langle W_i^{out}\rangle)$
Effect information (v_i)	the contribution of each node v_i to the network's EI	$EI_i = \mathrm{D}_{KL}[W_i^{out}\|\|\langle W_i^{out}\rangle]$
Micro-nodes in a macro-node	the set of micro-nodes grouped into a macro-node in the new network, G_M	$S = \{v_i, v_j, ...\}$, of length N_S
Macro-node out-weights	the out-weights from macro-node, μ, to its neighbors	$W_\mu^{out} = \sum_{i\in S} W_i^{out} \cdot \left(\frac{1}{N_S}\right)$
Macro-node out-weights given input weights	the out-weights from macro-node, μ, to its neighbors, *conditioned* on in-weights to the micro-nodes, $v_i \in S$	$W_{\mu\|j}^{out} = \sum_{i\in S} W_i^{out} \cdot \left(\frac{\sum_{j->i} w_{ji}}{\sum_{j->k\in S} w_{jk}}\right)$
Macro-node out-weights given the stationary distribution	the out-weights from macro-node, μ, to its neighbors, conditioned on the stationary probabilities, π_i, of micro-nodes, $v_i \in S$	$W_{\mu\|\pi}^{out} = \sum_{i\in S} W_i^{out} \cdot \left(\frac{\pi_i}{\sum_{k\in S}\pi_k}\right)$

TABLE I. **Table of key terms**. Quantities needed in order to calculate EI and create consistent macro-nodes.

in $W_i^{out} = \frac{1}{\langle k\rangle}$ and every value in $\langle W_i^{out}\rangle = \frac{\langle k\rangle}{N\langle k\rangle} = \frac{1}{N}$, which can be represented as:

$$EI_{ER} = \frac{1}{N}\sum_i^N \mathrm{D}_{KL}\Big[\big(\frac{1}{\langle k\rangle}, \frac{1}{\langle k\rangle}, ...\big)||\big(\frac{1}{N}, \frac{1}{N}, ...\big)\Big]$$

Each node in an ER network is expected to be identical to all other nodes in the network, and calculating the expected *effect information*, EI_i, is equivalent to calculating the network's EI. As such, we observe:

$$EI_i = \sum_{j=1}^{k_i} \frac{1}{\langle k\rangle} \cdot \log_2\left(\frac{\frac{1}{\langle k\rangle}}{\frac{1}{N}}\right) = \log_2\left(\frac{N}{pN}\right)$$

$$EI_{ER} = \frac{1}{N}\cdot\sum_i^N -\log_2(p) = -\log_2(p) \tag{10}$$

2. *Derivation: effective information of ring-lattice and star networks*

Here, we compare two classes of networks with the same average degree—ring lattice networks and star, or hub-and-spoke, graphs (see Fig. 8). In each network, we assume an average degree $\langle k\rangle = 2d$, with d being the dimension. The EI of star network, EI_{star}, approaches 0.0 as N gets larger, while the EI of ring lattices approaches $\log_2(N) - \log_2(2d)$. These derivations are shown below, first for the d-dimensional ring lattice, EI_d.

As every node in a ring lattice is connected to its $2d$ neighbors, each element of $\langle W_i^{out}\rangle$ is $\frac{1}{2d}$ and each element of W^{in} is $\frac{2d}{2d\times N} = \frac{1}{N}$.

$$EI_d = \frac{1}{N}\cdot\sum_i \mathrm{D}_{KL}\Big[\big(\frac{1}{2d}, \frac{1}{2d}, ...\big)||\big(\frac{1}{N}, \frac{1}{N}, ...\big)\Big] \tag{11}$$

Each node in a d-dimensional ring lattice is expected to be identical, so calculating the expected *effect information*, EI_i, is equivalent to calculating the network's EI. As such, we observe:

$$EI_i = \sum_{j=1}^{2d} \frac{1}{2d} \cdot \log_2\left(\frac{\frac{1}{2d}}{\frac{1}{N}}\right) = \log_2\left(\frac{N}{2d}\right)$$

$$EI_d = \log_2(N) - \log_2(2d) \tag{12}$$

Note: the EI of ring lattice networks reduces to simply the *determinism* of the network. The EI of ring lattice networks scale logarithmically with the size of the network, which is contrasted by the behavior of EI in star

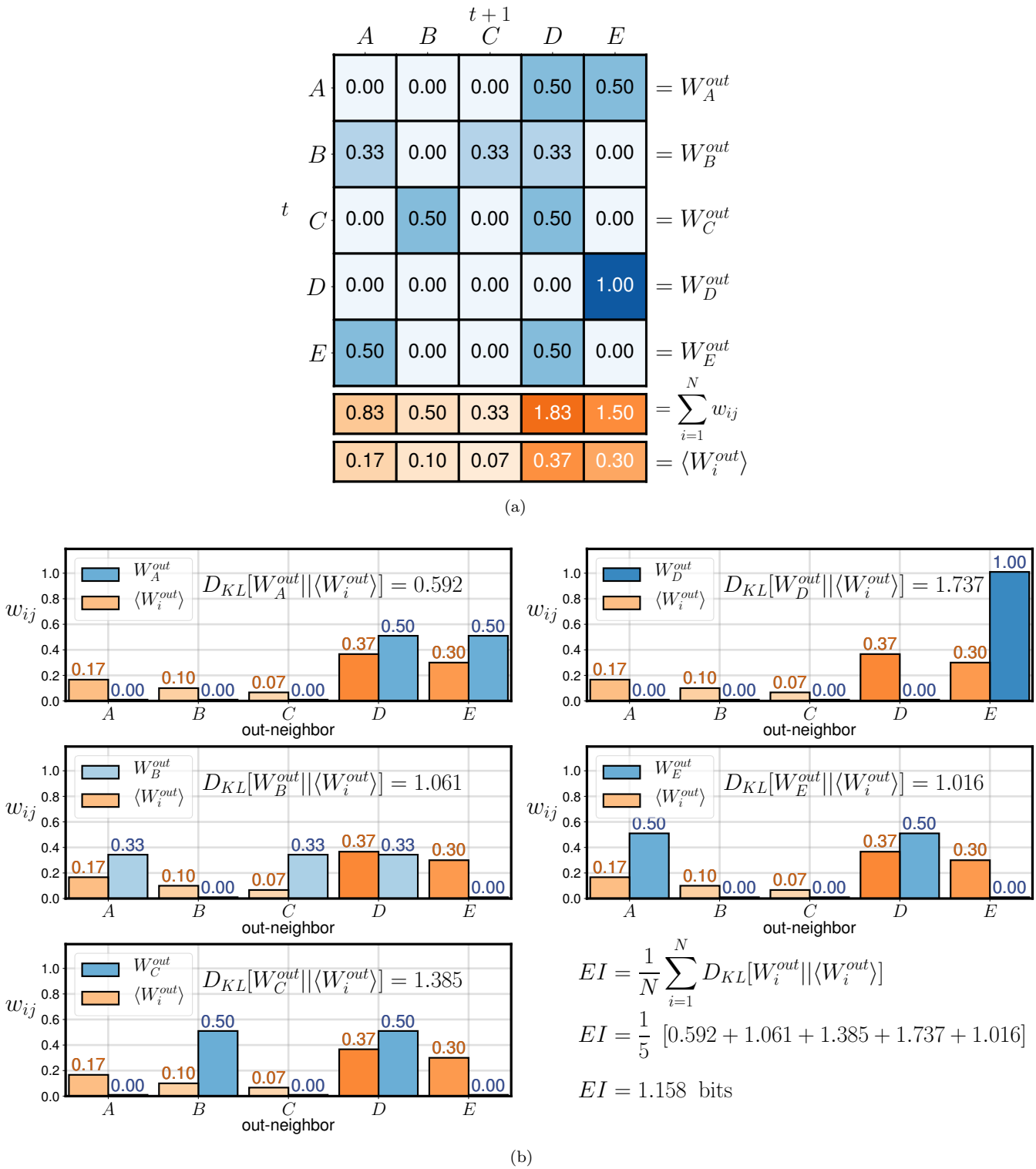

FIG. 7. **Illustration of the calculation of effective information.** (**A**) The adjacency matrix of a network with 1.158 bits of EI (calculation shown in (**B**)). The rows correspond to W_i^{out}, a vector of probabilities that a random walker on node v_i at time t transitions to v_j in the following time step, $t+1$. $\langle W_i^{out} \rangle$ represents the (normalized) input weight distribution of the network, that is, the probabilities that a random walker will arrive at a given node v_j at $t+1$, after a uniform introduction of random walkers into the network at t. (**B**) Each node's contribution to the EI (EI_i) is the KL divergence of its W_i^{out} vector from the network's $\langle W_i^{out} \rangle$, known as the *effect information*.

networks. Star networks have a hub-and-spoke structure, where $N-1$ nodes of degree $k_{spoke} = 1$ are connected

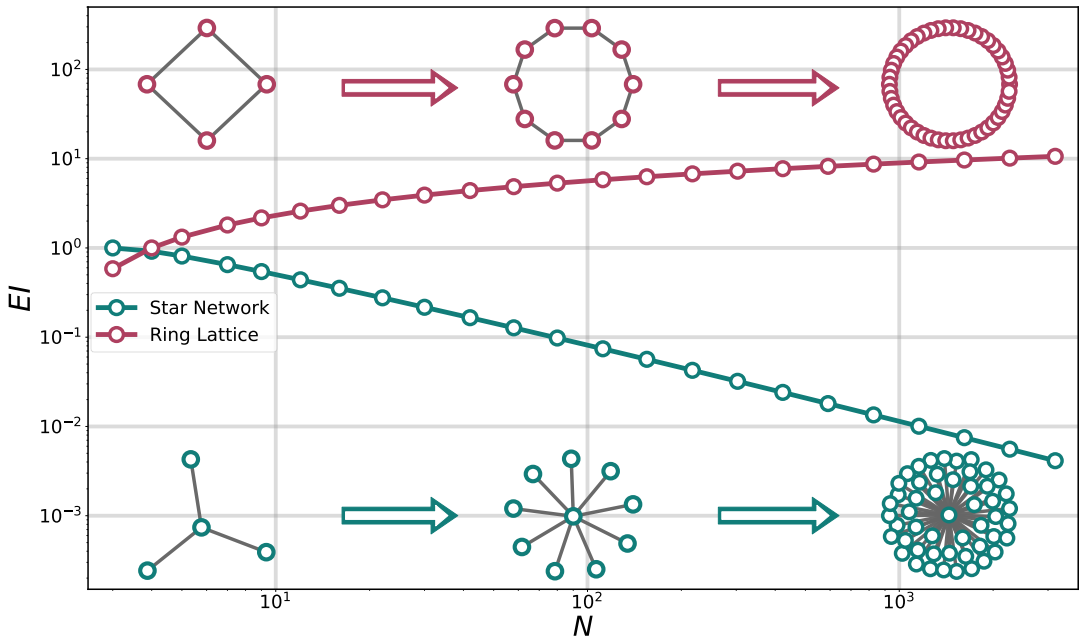

FIG. 8. **Effective information of stars and rings.** As the number of nodes in star networks increases, the EI approaches zero, while the EI of ring lattice networks grows logarithmically as the number of nodes increases.

a hub node, which itself has degree $k_{hub} = N - 1$. For star networks, EI approaches 0.0 as the number of nodes increases. This derivation is shown below.

$$EI_{star} = \frac{1}{N} \cdot \left[\sum_{i=1}^{N-1} \mathrm{D}_{KL} \left[W_{spoke}^{out} || \langle W_i^{out} \rangle \right] + \mathrm{D}_{KL} \left[W_{hub}^{out} || \langle W_i^{out} \rangle \right] \right]$$

Every spoke has an out-weight vector W_i^{out} with $N-1$ elements of $w_{ij} = 0.0$ and one with $w_{ij} = 1.0$. The single hub, however, has $N - 1$ elements of $w_{ij} = \frac{1}{N-1}$ with a single $w_{ij} = 0.0$. Similarly, $\langle W_i^{out} \rangle$ consists of $N - 1$ elements with values $\frac{1}{N(N-1)}$.

$$EI_{star} = \frac{1}{N} \cdot \left[\sum_{i=1}^{N-1} \mathrm{D}_{KL} \left[\frac{1}{1} || \frac{N-1}{N} \right] + \mathrm{D}_{KL} \left[\frac{1}{N-1} || \frac{1}{N(N-1)} \right] \right] \quad (13)$$

Using the same techniques as above, this equation reduces to:

$$EI_{star} = \frac{1}{N} \cdot \left[(N-1) \cdot \log_2 \left(\frac{\frac{1}{1}}{\frac{(N-1)}{N}} \right) + \log_2 \left(\frac{\frac{1}{N-1}}{\frac{1}{N(N-1)}} \right) \right]$$

$$EI_{star} = \frac{N-1}{N} \cdot \log_2 \left(\frac{N}{N-1} \right) + \frac{1}{N} \cdot \log_2 (N)$$

$$EI_{star} = 0.0 \text{ as } \lim_{N \to \infty} \quad (14)$$

D. Network motifs as causal relationships

It is important to understand why certain motifs have more EI while others have less. In Fig. 9, we show the EI in 13 directed three-node network motifs. The connectivity of each motif drastically influences the EI. Motif 09—the directed cycle—is the motif with the highest EI. Intuitively, this fits with our definition of EI: the amount of certainty in the network (notably, each link in Motif 09, if taken to represent a causal relationship, is both necessary and sufficient). A random walker in this system has zero entropy (even if the direction of its path were reversed), whereas every other three-node motif does not contain that degree of certainty. Second, we see that Motif 04—a system with a "sink" node—has

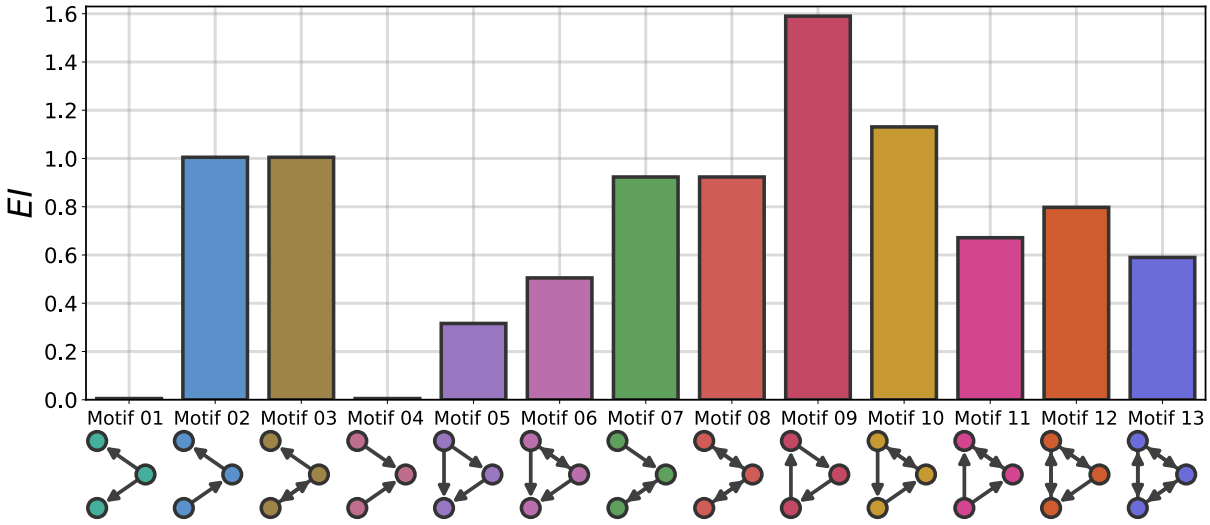

FIG. 9. **Effective Information of network motifs.** All directed 3-node subgraphs and their EI.

no EI, suggesting that a causal structure with that architecture is not informative, since all causes lead to the same effect. Similarly, because there are no outputs from two nodes in Motif 01, we see an EI value of zero.

E. Table of network data

In Table II, we report the name, domain, source, category, and description of each of the 84 networks used in our comparison of EI in real networks. These networks were selected primarily from the Konect database [23], with supplemental datasets added from NetworkRepository [24] when the Konect database lacked a sufficient number of datasets in a given category, since the two databases already significantly overlapped. In many cases, the interactions among nodes in these networks (i.e., their edges) can reasonably be interpreted as causal, directed influence, or dependencies such that the behavior of a node, v_i, at a given time can be thought to impact the behavior of its neighbors, v_j. By instituting relatively minimal requirements for selecting the above networks, we are able to assess the EI in a variety of complex systems across different domains. However, while we can measure the EI of any given network, the further interpretation of this EI depends also on what the nodes and edges of a network represent. In a case where the nodes represent states of a system, such as a Markov process, then the EI directly captures the information in the causal structure. In the case where the nodes represent merely dependencies or influence, EI can still be informative as a metric to compare different networks. In a network specifically composed of non-causal correlations, then EI is merely a structural property of the network's connectivity.

F. Examples of consistent macro-nodes

In Fig. 11 we display 15 different parameterizations of small networks grown under degree-based preferential attachment. Each plot shows to the inconsistency of the mapping from the microscale to the macroscale, in bits, which corresponds to the KL divergence of the distribution of random walkers on microscale nodes and the same distribution at the macroscale. Each of these networks are consistent after 1000 timesteps, with eight showing full consistency from the start. These 15 example networks also show the range of causal emergence values that is found in networks.

G. Emergent subgraphs

What sort of subgraph connectivity leads to causal emergence? To explore this we take two independent subgraphs, and couple them together while varying their size, moving from clique-like to bipartite connectivity. We then check to see if grouping those clusters into macro-nodes leads to causal emergence (Fig. 12). Specifically, we simulate many small unweighted, undirected networks ($N = 100$) from a stochastic block model with two clusters, and we vary the probability of within-cluster edges (from 0.0 to 1.0) as well as the size-asymmetry of the two clusters (illustrated around the border of Fig. 12). In each simulation, we group the microscale network into two macro-nodes, each corresponding to one cluster. What we observe is a causal emergence landscape with several important characteristics (Fig. 12). First, in these networks we observe causal emergence when the fraction of within-cluster connections is either very high or very low (right and left sides of the heatmap in Fig. 12). These are the conditions in which there is a large

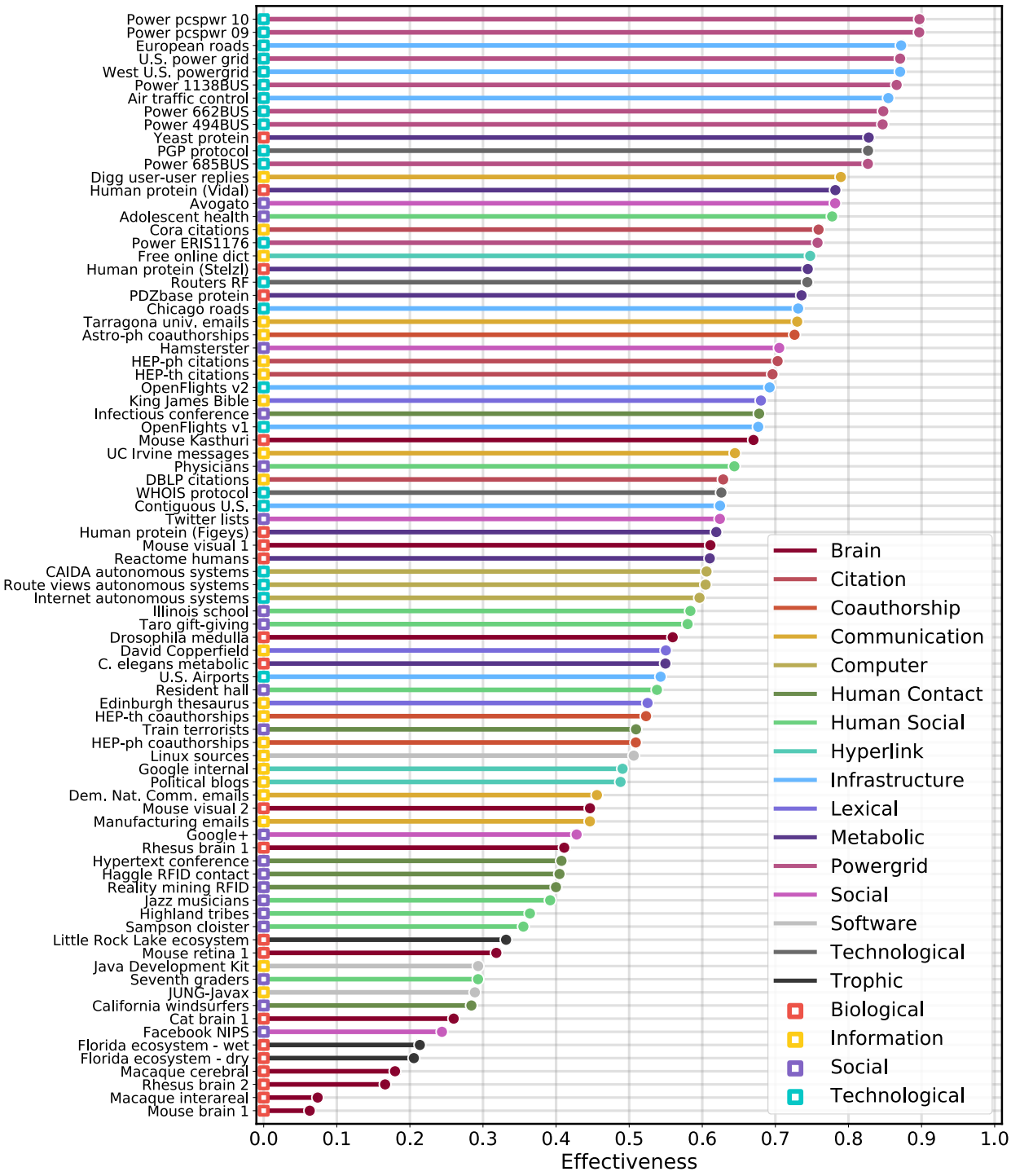

FIG. 10. **Effectiveness of real networks.** Full data behind the results summarized in Fig. 3, color-coded in two ways. First by 16 "Domains" (as in Table II), which corresponds to the classification of each network from its source repository (in this case, the Konect database [23] or the Network Repository [24]). The second categorization we report—those used in Fig. 3—involves grouping the Domains into four "Categories" ("Cat." in Table II): Biological, Information, Social, and Technological. These correspond to the colored squares to the right of each network's name.

amount of uncertainty, or noise, in that subgraph. Not only that, however, causal emergence is most likely when there is a size asymmetry between the two clusters, suggesting that macroscales that maximize a network's EI often do so by creating a more evenly distributed $\langle W_i^{out} \rangle$. In general, however, the space of subgraphs leans toward

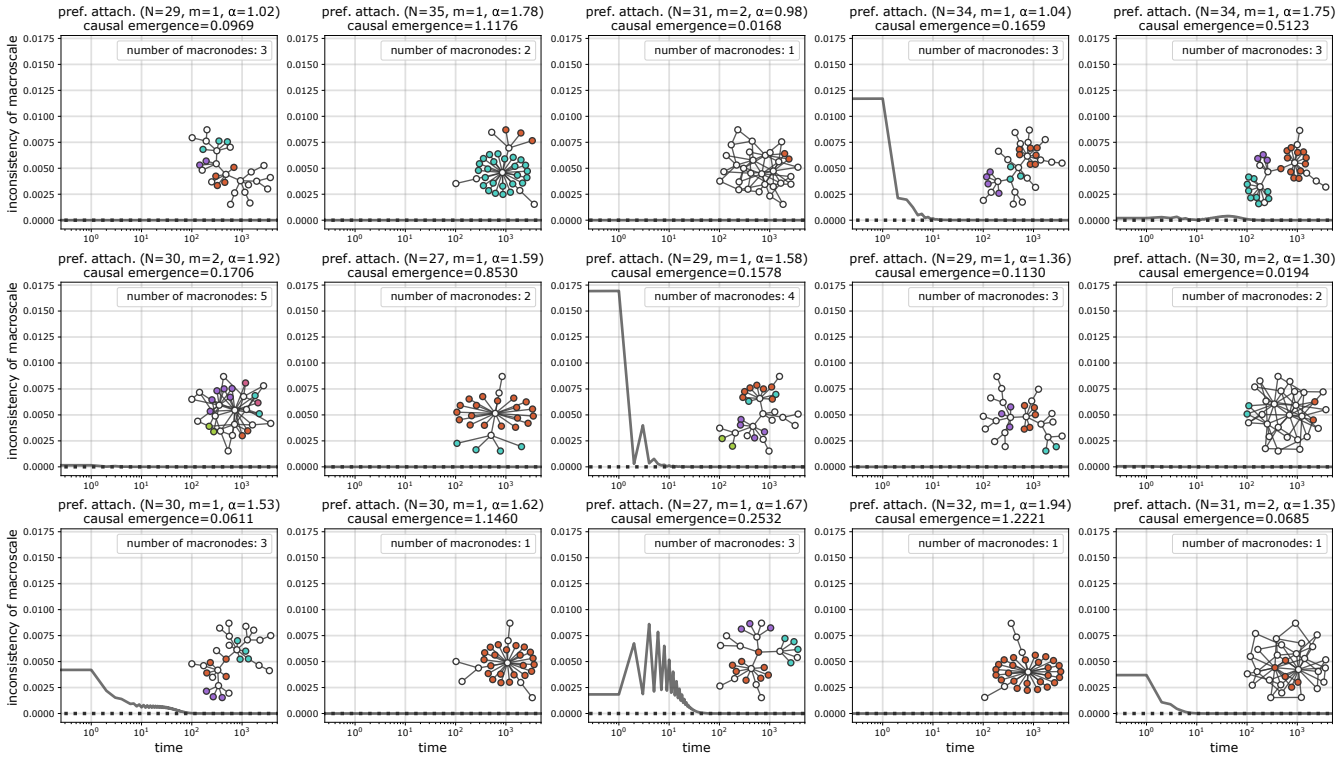

FIG. 11. **Typically minimal inconsistency of higher-order macro-nodes.** Each inset is of the microscale network, where each node's color corresponds to the $\mu|\pi$ macro-node it has been mapped to following one instance of the greedy algorithm detailed in the Materials & Methods section. White nodes indicate a micro-node that was not grouped into a new macro-node. Inconsistency is plotted over time.

causal reduction (a loss of EI after grouping), which fits with the success of reduction historically and explains why researchers and modelers should generally be biased toward reduction.

In cases of complete noise, with no asymmetries or differences between intra- or inter-connectivity between subgraphs, we should expect causal emergence to be impossible. Indeed, this is what we see for many parameterizations of Erdős-Rényi networks of various sizes (Fig. 13). This result follows from insights in Fig. 1a, where the EI of ER networks converges to a fixed value of $-\log_2(p)$ as the size of the network increases. Here, we observe some causal emergence in ER networks but only when the networks are very small. Importantly, the amount of causal emergence is also very small, especially relative to the causal emergence in networks with preferential attachment. This further suggests that causal emergence moves the existent structure of the network into focus by examining the network at a certain scale, rather than creating that structure from nothing.

Network name	Domain	Source	Cat.	Description
HEP-th citations	Citation	Konect	Inf.	high-energy physics (HEP) citations - theory
HEP-ph citations	Citation	Konect	Inf.	HEP citations - phenomenology
Cora citations	Citation	Konect	Inf.	citations from the Cora database
DBLP citations	Citation	Konect	Inf.	database of scientific publications
Astro-ph coauthorships	Coauthorship	Konect	Inf.	coauthors on astronomy arXiv papers
HEP-th coauthorships	Coauthorship	Konect	Inf.	coauthors on HEP-theory arXiv papers
HEP-ph coauthorships	Coauthorship	Konect	Inf.	coauthors on HEP-phenomenology arXiv papers
Tarragona univ. emails	Communication	Konect	Soc.	emails from the University Rovira i Virgili
Dem. Nat. Comm. emails	Communication	Konect	Soc.	2016 Democratic National Committee email leak
Digg user-user replies	Communication	Konect	Soc.	reply network from the social news website Digg
UC Irvine messages	Communication	Konect	Soc.	messages between students at UC Irvine
Manufacturing emails	Communication	Konect	Soc.	internal emails between employees at a company
CAIDA autonomous systems	Computer	Konect	Tec.	autonomous systems network from CAIDA, 2007
Route views autonomous systems	Computer	Konect	Tec.	autonomous systems network
Internet autonomous systems	Computer	Konect	Tec.	connected IP routing
Haggle RFID contact	Human Contact	Konect	Soc.	human proximity, via carried wireless devices
Reality mining RFID	Human Contact	Konect	Soc.	RFID data from 100 MIT students' interactions
California windsurfers	Human Contact	Konect	Soc.	contacts between windsurfers California, 1986
Train terrorists	Human Contact	Konect	Soc.	contacts between Madrid train bombing suspects
Hypertext conference	Human Contact	Konect	Soc.	face-to-face contacts at the ACM Hypertext 2009
Infectious conference	Human Contact	Konect	Soc.	face-to-face contacts at INFECTIOUS, 2009
Jazz musicians	Human Social	Konect	Soc.	collaboration network between Jazz musicians
Adolescent health	Human Social	Konect	Soc.	surveyed students list their best friends
Physicians	Human Social	Konect	Soc.	innovation spread network among 246 physicians
Resident hall	Human Social	Konect	Soc.	friendship ratings between students in a dorm
Sampson cloister	Human Social	Konect	Soc.	relations between monks in a monastery
Seventh graders	Human Social	Konect	Soc.	proximity ratings between seventh grade students
Taro gift-giving	Human Social	Konect	Soc.	gift-givings (taro) between households
Dutch college	Human Social	Konect	Soc.	friendship ratings between university freshmen
Highland tribes	Human Social	Konect	Soc.	tribes in the Gahuku-Gama alliance structure
Illinois school	Human Social	Konect	Soc.	friendships between boys at an Illinois highschool
Free online dict.	Hyperlink	Konect	Inf.	cross references in Free Online Dict. of Computing
Political blogs	Hyperlink	Konect	Inf.	hyperlinks between blogs, 2004 US election
Google internal	Hyperlink	Konect	Inf.	hyperlink network from pages within Google.com
Air traffic control	Infrastructure	Konect	Tec.	USA's FAA, Preferred Routes Database
OpenFlights v1	Infrastructure	Konect	Tec.	flight network between airports, OpenFlights.org
OpenFlights v2	Infrastructure	Konect	Tec.	flight network between airports, OpenFlights.org
Contiguous U.S.	Infrastructure	Konect	Tec.	48 contiguous states and D.C. of the U.S.
European roads	Infrastructure	Konect	Tec.	international E-road network, mainly in Europe
Chicago roads	Infrastructure	Konect	Tec.	road transportation network of the Chicago region
West U.S. powergrid	Infrastructure	Konect	Tec.	power grid of the Western U.S.
U.S. Airports	Infrastructure	Konect	Tec.	flights between US airports in 2010
David Copperfield	Lexical	Konect	Inf.	network of common noun and adjective adjacencies
Edinburgh thesaurus	Lexical	Konect	Inf.	word association network, collected experimentally
King James Bible	Lexical	Konect	Inf.	co-occurrence between nouns in the Bible

TABLE II. **Network datasets.** Continued on the following page.

Network name	**Domain**	**Source**	**Cat.**	**Description**
C. elegans metabolic	Metabolic	Konect	Bio.	metabolic network of the *C. elegans* roundworm
Human protein (Figeys)	Metabolic	Konect	Bio.	interactions network of proteins in Humans
PDZbase protein	Metabolic	Konect	Bio.	protein-protein interactions from PDZBase
Human protein (Stelzl)	Metabolic	Konect	Bio.	interactions network of proteins in Humans
Human protein (Vidal)	Metabolic	Konect	Bio.	proteome-scale map of Human protein interactions
Yeast protein	Metabolic	Konect	Bio.	protein interactions contained in yeast
Reactome humans	Metabolic	Konect	Bio.	protein interactions, from the Reactome project
Avogato	Social	Konect	Soc.	trust network for users of Advogato
Google+	Social	Konect	Soc.	Google+ user-user connections
Hamsterster	Social	Konect	Soc.	friendships between users of hamsterster.com
Twitter lists	Social	Konect	Soc.	Twitter user-user following network
Facebook NIPS	Social	Konect	Soc.	Facebook user-user friendship network
Linux dependency	Software	Konect	Inf.	Linux source code dependency network
J.D.K. dependency	Software	Konect	Inf.	software class dependencies, JDK 1.6.0.7
JUNG/javax dependency	Software	Konect	Inf.	software class dependencies, JUNG 2.0.1 & javax
Florida ecosystem - dry	Trophic	Konect	Bio.	food web in the Florida wetlands (dry season)
Florida ecosystem - wet	Trophic	Konect	Bio.	food web in the Florida wetlands (wet season)
Little Rock Lake ecosystem	Trophic	Konect	Bio.	food web of Little Rock Lake, Wisconsin
WHOIS protocol	Technological	NetworkRepository	Tec.	dataset of internet routing registries
PGP protocol	Technological	NetworkRepository	Tec.	trust protocol of private keys of internet users
Routers RF	Technological	NetworkRepository	Tec.	traceroute network between routers via Rocketfuel
Cat brain 1	Brain	NetworkRepository	Bio.	fiber tracts between brain regions of a cat
Drosophila medulla	Brain	NetworkRepository	Bio.	neuronal network from the medulla of a fly
Rhesus brain 1	Brain	NetworkRepository	Bio.	collation of tract tracing studies in primates
Rhesus brain 2	Brain	NetworkRepository	Bio.	inter-areal cortical networks from a primate
Macaque cerebral	Brain	NetworkRepository	Bio.	connections between cerebral cortex of a primate
Macaque interareal	Brain	NetworkRepository	Bio.	inter-areal cortical networks from a primate
Mouse Kasthuri	Brain	NetworkRepository	Bio.	neuronal network of a mouse
Mouse brain 1	Brain	NetworkRepository	Bio.	calcium imaging of neuronal networks in a mouse
Mouse retina 1	Brain	NetworkRepository	Bio.	electron microscopy of neurons in mouse retina
Mouse visual 1	Brain	NetworkRepository	Bio.	electron microscopy of visual cortex of a mouse
Mouse visual 2	Brain	NetworkRepository	Bio.	electron microscopy of visual cortex of a mouse
Power 1138BUS	Powergrid	NetworkRepository	Tec.	power system admittance, via Harwell-Boeing
Power 494BUS	Powergrid	NetworkRepository	Tec.	power system admittance, via Harwell-Boeing
Power 662BUS	Powergrid	NetworkRepository	Tec.	power system admittance, via Harwell-Boeing
Power 685BUS	Powergrid	NetworkRepository	Tec.	power system admittance, via Harwell-Boeing
U.S. power grid	Powergrid	NetworkRepository	Tec.	electricity / power transmission network in the U.S.
Power pcspwr 09	Powergrid	NetworkRepository	Tec.	BCSPWR09 powergrid data via Harwell-Boeing
Power pcspwr 10	Powergrid	NetworkRepository	Tec.	BCSPWR10 powergrid data via Harwell-Boeing
Power ERIS1176	Powergrid	NetworkRepository	Tec.	powergrid data via Erisman, 1973

TABLE II. **Network datasets (continued).**

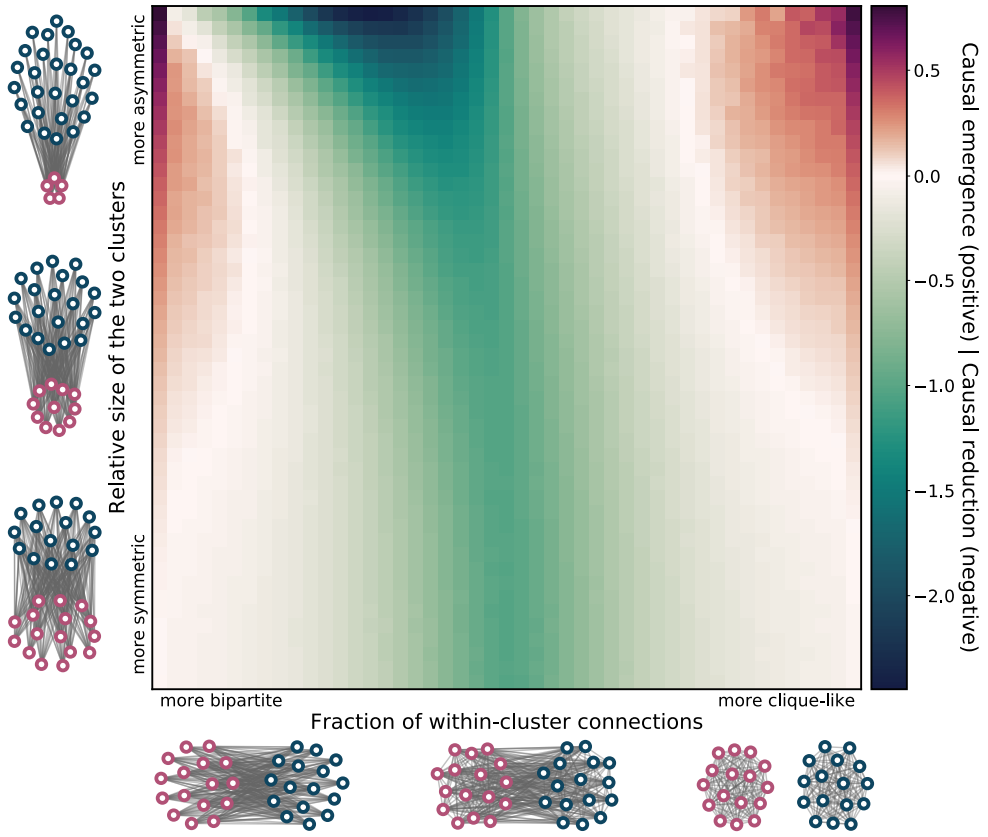

FIG. 12. **Causal emergence in a simplified stochastic block model.** Schematic showing the role of the two relevant parameters—the fraction of nodes in each community (ranging from $r = 0.50$ to $r < 1.0$) and the fraction of within-cluster connections (ranging from $p = 0.0$, a fully bipartite network, to $p = 1.0$—two disconnected cliques). By repeatedly simulating networks under various combinations of parameters ($N = 100$ with 100 simulations per combination of parameters), we see combinations that are more apt to produce networks with causal emergence.

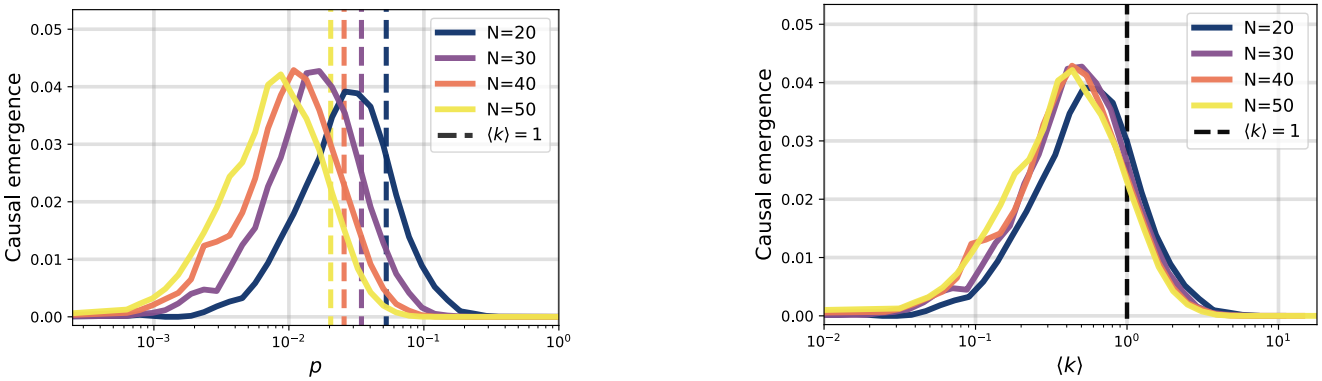

(a) (b)

FIG. 13. **Causal emergence in Erdős-Rényi networks.** (**A**) As the edge density, p, of ER networks increases and N is held constant, the amount of causal emergence quickly drops to zero. (**B**) This drop occurs well before $pN = \langle k \rangle = 1$, meaning the algorithm for uncovering causal emergence is only grouping small, disconnected, tree-like subgraphs that have yet to form into a giant component. Of note here is the low magnitude of causal emergence even in cases where the random network is not a single large component, and the vanishing of causal emergence after it is.